

A 28-GHz High-Gain Slotted Array Antenna with Beam Steering Capability for 5G Millimeter-Wave Applications

Thura Ali Khalaf* and Gölge Ögücü Yetkin

Department of Electrical and Electronics Engineering, Gaziantep University, Gaziantep – 27310, Turkey

**E-mail: thuraalikhalaf@gmail.com*

ABSTRACT

To address the common issues associated with using high-frequency millimeter bands in fifth generation (5G) communication, it is crucial to develop an efficient, high-gain, and beam-steerable antenna system. This study proposes a simple array structure consisting of 10 U-shaped slotted patches operating at 28 GHz. The single-element antenna offers good radiation characteristics with a gain of 8.4 dBi and a radiation efficiency of over 95 % at 28 GHz. The slots of the patch demonstrate strong performance in terms of resonant frequency, gain, and total efficiency. Both the single-element and the array antennas have a reflection coefficient of ≤ -10 dB at the resonating frequency and a good 10-dB bandwidth that covers the entire 5G (27.5–28.35 GHz) band. To increase the gain, the antenna element is transformed into a 1×10 array. As a result, the peak gain of the array was successfully boosted to 18.5 dBi with 95 % radiation efficiency at the working frequency. The simulations show that the proposed array can cover up to $\pm 44^\circ$ with a minimum gain of 14.8 dBi. At the maximum steering angle, the array achieved 94 % radiation efficiency and 91 % total efficiency. Overall, the proposed antenna array demonstrates high performance in terms of gain, efficiency, and beam-steering characteristics, making it a strong candidate for use in upcoming 5G communication systems.

Keywords: 5G; Millimeter-wave; 28-GHz; Microstrip patch antenna; Phased array antenna

1. INTRODUCTION

Mobile communication technologies are evolving rapidly to fulfill the requirements of the fifth generation (5G). One of the frequency bands that satisfies these demands is the millimeter-wave. Utilising this spectrum makes a 5G communication system capable of reaching high data rates. However, working in this high-frequency band is subject to high losses, but such losses can be mitigated by installing antenna array systems at the transmitter and receiver ends¹⁻⁴.

The Federal Communications Commission (FCC) of the United States and the European Union (EU) have announced that the 24–28.5 GHz band is a potential candidate for the 5G millimeter-wave spectrum. The 28 GHz frequency band, which has been designated as an experimental band in several countries, is considered an excellent candidate for 5G communication. However, this high-frequency band is susceptible to high propagation loss due to atmospheric absorption, which can negatively impact signal quality at the receiving terminals. According to the Friis transmission formula, as the resonant frequency increases, the wavelength becomes shorter, resulting in higher losses. Therefore, effective antenna designs that meet the 5G requirements are crucial for 5G millimeter-wave communication systems⁵⁻⁸.

The antenna systems used in 5G applications should be compact, with high gain and directivity⁹. High-gain antenna designs must be utilised to overcome atmospheric losses and

ensure reliable service at the receiver end¹⁰⁻¹¹. The most effective approach to designing a high-gain antenna is to employ an array of antennas, as this increases the gain in proportion to the number of elements in the array. However, in certain applications, such as mobile phones, space is limited, making it difficult to increase the number of elements in the array. As a result, designing low-profile, high-gain array antennas presents a significant challenge.

To achieve wide spatial communication coverage and reliable connections in complicated environments, it is necessary to have a high steering angle for beam steering capability. One effective technique for implementing this is the use of phased array antennas. These arrays can be created by aligning the antennas in either a planar or a linear fashion. The primary purpose of phased array antennas is to steer the main beam by employing a phase shifter on each element to delay signals as they leave the antenna elements. By controlling the port amplitude and phase of the array units, the combined radiations from all the elements form a beam that is accurately pointed in the desired direction with high gain and fewer losses. Therefore, to address the challenges of the high-frequency millimeter-wave band, it is crucial to develop novel phased array antennas with a high gain, large scanning angle, and compact design for 5G cellular communication because of their capability to enhance the efficiency and connectivity of 5G systems¹²⁻¹⁶.

Recent studies have focused on designing linear high-gain antenna arrays with beam steering capabilities at 28 GHz. Authors proposed a 1×8 quasi-yagi slotted array antenna with

a peak gain of 11.16 dBi and coverage of $\pm 48^\circ$ by using the progressive phase shift method with a uniform amplitude between the elements¹². However, this gain value falls short of the minimum requirement of 12 dBi for 5G communication, which is necessary to overcome path loss at millimeter-wave frequencies¹⁷. Another study¹⁸ reported an eight-element T-shaped slot array with single directors, achieving a maximum gain of 12.5 dBi and a steering angle of 70° . Similarly, another study¹⁹ used an eight-dipole antenna array design with a peak scan angle of 80° at 25–36 GHz, also achieving a gain of 12.5 dBi. A 10-patch array was proposed, achieving a maximum gain of 12.8 dBi and a wide steerable angle of 121° in the broadside direction¹⁴.

However, during the beam-steering mechanism, the gains suffered from variations of 4.5, 1.5, and 3 dB, respectively, causing them to drop below the required 5G gain at certain steering angles^{14,18–19}. The authors presented a 1×8 patch array with a peak gain of 14.4 dB and a wide scanning angle of $\pm 70^\circ$ with less than 3 dBi gain loss at 26.5 GHz²⁰. An array of 32

inverted-F patches achieved a high gain of 16.52 dB at 28.38 GHz and a coverage of $\pm 45^\circ$ ²¹. However, the array had a small bandwidth of only 890 MHz at 28 GHz, which is insufficient for 5G mobile applications, as it must have at least a 1 GHz 10-dB bandwidth²². The researchers proposed a capacitive coupled patch antenna array that consists of 12 elements²³. The array achieved a high gain of around 16.5 dBi, with $\pm 60^\circ$ steering coverage at 24–28 GHz.

After reviewing recent reports on 5G antennas, it is clear that further development in designing antennas with improved gain performance and beam steering capabilities is required to reduce path loss at millimeter-wave frequencies. This study aims to address this issue by designing a high-gain antenna array with beam steering capability operating at 28 GHz. The array consists of a rectangular microstrip patch with two U-shaped slots as a single-element. To increase the gain, the single-element is transformed into a 10-element array using the Computer Simulation Technology (CST) solver. For beam steering, each feed port of the array is connected to a phase

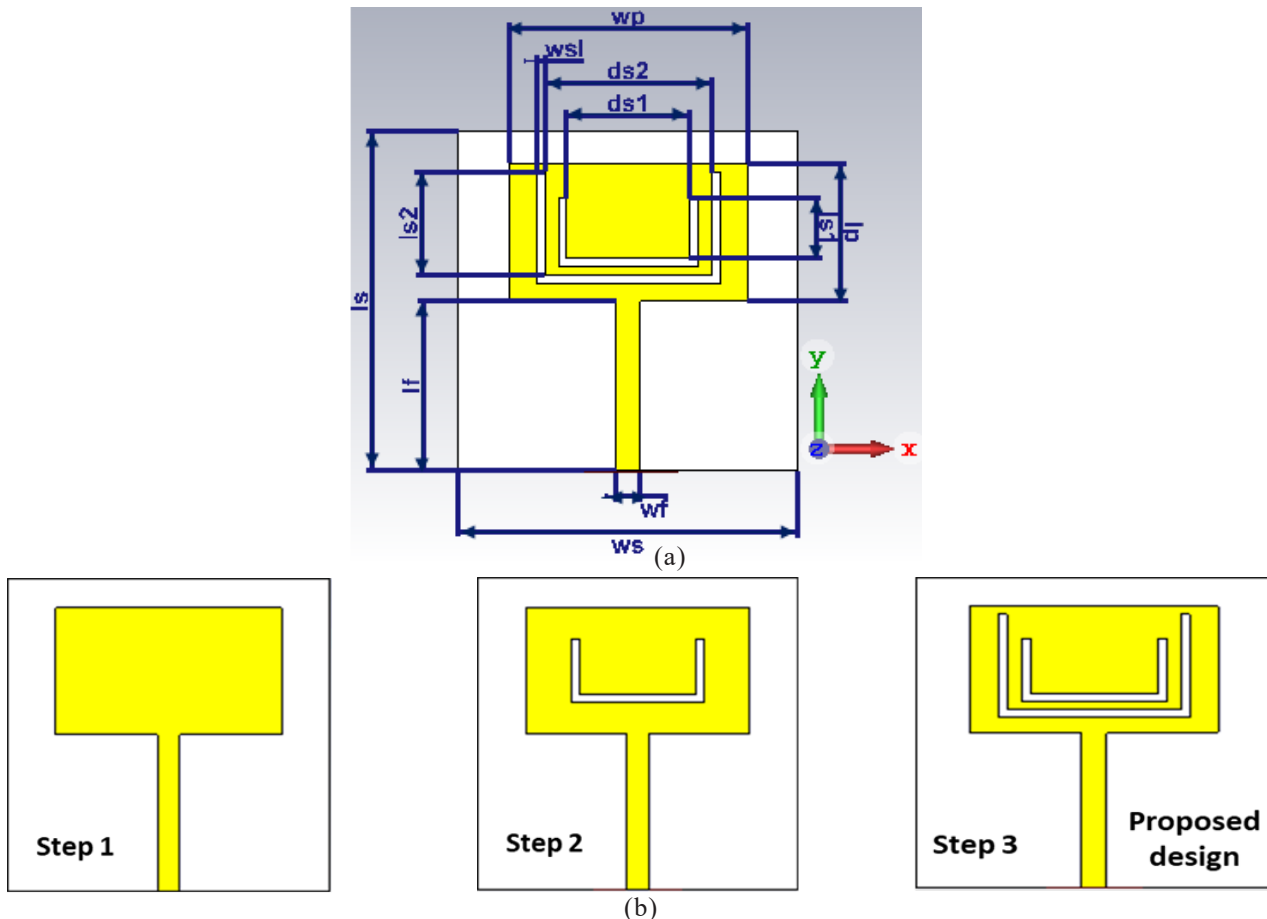


Figure 1. Proposed antenna element; (a) Geometry; and (b) Design steps.

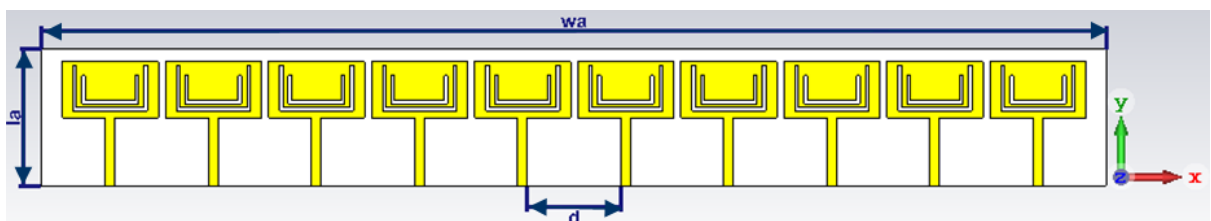


Figure 2. Proposed array antenna.

shifter, allowing for different phase shifts to be applied to each element. The proposed array is then simulated to demonstrate its high gain, efficiency, and beam-steering performance at various scanning angles.

2. ANTENNA DESIGN

Figure 1(a) illustrates the structure of a single-element antenna. The main objective of this research is to create a high-gain antenna for which a Rogers RT5880 substrate with a dielectric constant of 2.2 and a loss tangent of 0.0009 is utilised. The Rogers material typically has lower losses, making it ideal for high-frequency 5G applications that require high gain⁹. The substrate layer has dimensions of $w_s \times l_s$ mm² with a thickness of 0.51 mm. The patch dimension is $w_p \times l_p$ mm², and the transmission line is $w_f \times l_f$ mm². The patch and transmission line are printed together on top of the substrate. The single microstrip antenna features double U-shaped slots located within the patch. These slots are incorporated into the design to achieve resonance at the desired frequency and to improve radiation properties. Table 1 outlines the parameters of the single-element. Figure 1(b) displays the progression of the design steps for the proposed double-slotted antenna.

The proposed array antenna is composed of 10 doubly U-shaped slotted patches with an overall dimension of $w_a \times l_a$ mm². Table 2 lists the dimensions for the 10-element array. The antennas are evenly spaced and arranged in a straight line along the x-axis, as illustrated in Fig. 2. The interelement spacing of the proposed array is 6.80 mm, which falls within the standard range of 0.5λ – 0.9λ ⁶.

Table 1. Parameter list of the antenna element

Parameter	Dimension (mm)
ls	10
ws	10
lp	4.05
wp	7
ds1	3.6
ds2	4.9
ls1	1.75
ls2	3.05
wsl	0.25
wf	0.7
lf	5

Table 2. Parameter list of the array antenna

Parameter	Dimension (mm)
la	10
wa	77.5
d	6.80

3. BEAM-STEERING ANALYSIS

Before conducting a beam-steering investigation of the proposed array, a phase shift was applied to all ports except the first one, which remained at zero throughout the process. For a 10-element phased array antenna, the phase shift assignment was as follows:

$$\varnothing_N = N\varnothing \quad (1)$$

where $N = 0, 1, 2, \dots, 9$, and \varnothing is the assigned phase shift, and \varnothing_N is the phase shift function.

If we set \varnothing to 100° , the phase shifts of the array units will be $0^\circ, 100^\circ, 200^\circ, \dots$, and 900° for the first, second, third, ..., and tenth elements, respectively. Throughout the testing process, the amplitude was kept constant. Once the phase and amplitude were assigned, the resulting far-field radiation pattern was observed. Therefore, the array factor for the proposed linear array can be expressed as follows:

$$AF = \sum_{n=0}^N A_n e^{j\varnothing_N} \quad (2)$$

where, A is the amplitude, which has a value of 1 for all elements.

Therefore, the AF expression becomes as follows:

$$AF = \sum_{n=0}^9 A_n e^{j\varnothing_N} = 1 + e^{j\varnothing_1} + \dots + e^{j\varnothing_9} \quad (3)$$

4. DISCUSSION AND SIMULATION RESULTS

4.1 Single Element

This section presents the primary simulation results for the single-element antenna design, as illustrated in Fig. 3. Figure 3(a) shows the reflection coefficient for each design step. The proposed patch achieved a return loss of -21.6 dB at 28.3 GHz, while the other patch designs resonate at different frequency bands. This indicates that the addition of two slots allows the antenna to resonate at the desired frequency with low loss. The 10-dB bandwidth in this case is above 2 GHz, which effectively covers the entire 5G band (27.5–28.35 GHz)⁶.

Figure 3(b) compares the gain characteristics of the single-element antenna designs over frequency. Figure 3(c) presents the far-field 3D radiation pattern for the patch designs, which can be used to analyze the radiation characteristics of a single-element antenna. Both figures clearly demonstrate the impact of slots on the gain. By comparing the gain performance of the patch designs, it is evident from the figures that the proposed antenna achieved a maximum gain value of 8.4 dBi at 28 GHz. The unslotted and single-slotted patches obtained gain values of 6.5 and 7.9 dBi, respectively, at 28 GHz.

The directivity of the single-patch antenna was approximately 8.6 dBi, indicating excellent directional performance. Additionally, the single-element antenna exhibited a high realised gain value of 8.3 dBi. The proposed patch radiated at an angle of 9° with a side lobe level of -15.4 dB in the theta ($\phi = 90^\circ$) direction. The proposed solo patch also boasted a radiation efficiency of more than 95 % (-0.2115 dB) and a total efficiency of almost 94 % (-0.2834) at the resonant frequency, indicating that it effectively radiates most of the input power. When an antenna is connected to a transmission line, its total efficiency is calculated by multiplying its radiated efficiency by the antenna's mismatch loss. The total efficiency can be expressed as follows²²:

$$\hat{\epsilon}_t = \epsilon_a \times \epsilon_r \quad (4)$$

where, ϵ_t is the total efficiency, ϵ_a is the antenna loss, and ϵ_r is the radiation efficiency. The value of ϵ_a usually ranges from 0 to 1. The unslotted patch showed a total efficiency of almost 77 % (-1.125 dB), and the single-slotted patch demonstrated a total efficiency of 87.5 % (-0.5792 dB) at 28 GHz. Including slots

in the single element positively impacts the total efficiency, as illustrated in Fig. 3(c). Therefore, due to the favorable effect of the slots on the patch, the double-slotted patch was selected as a single element for the array antenna.

4.2 Array Antenna

Before beginning the simulation process, each element was excited with the same amplitude and a progressive phase shift based on its location in the array. The results were then combined to investigate the beam-steering mechanism. Figure

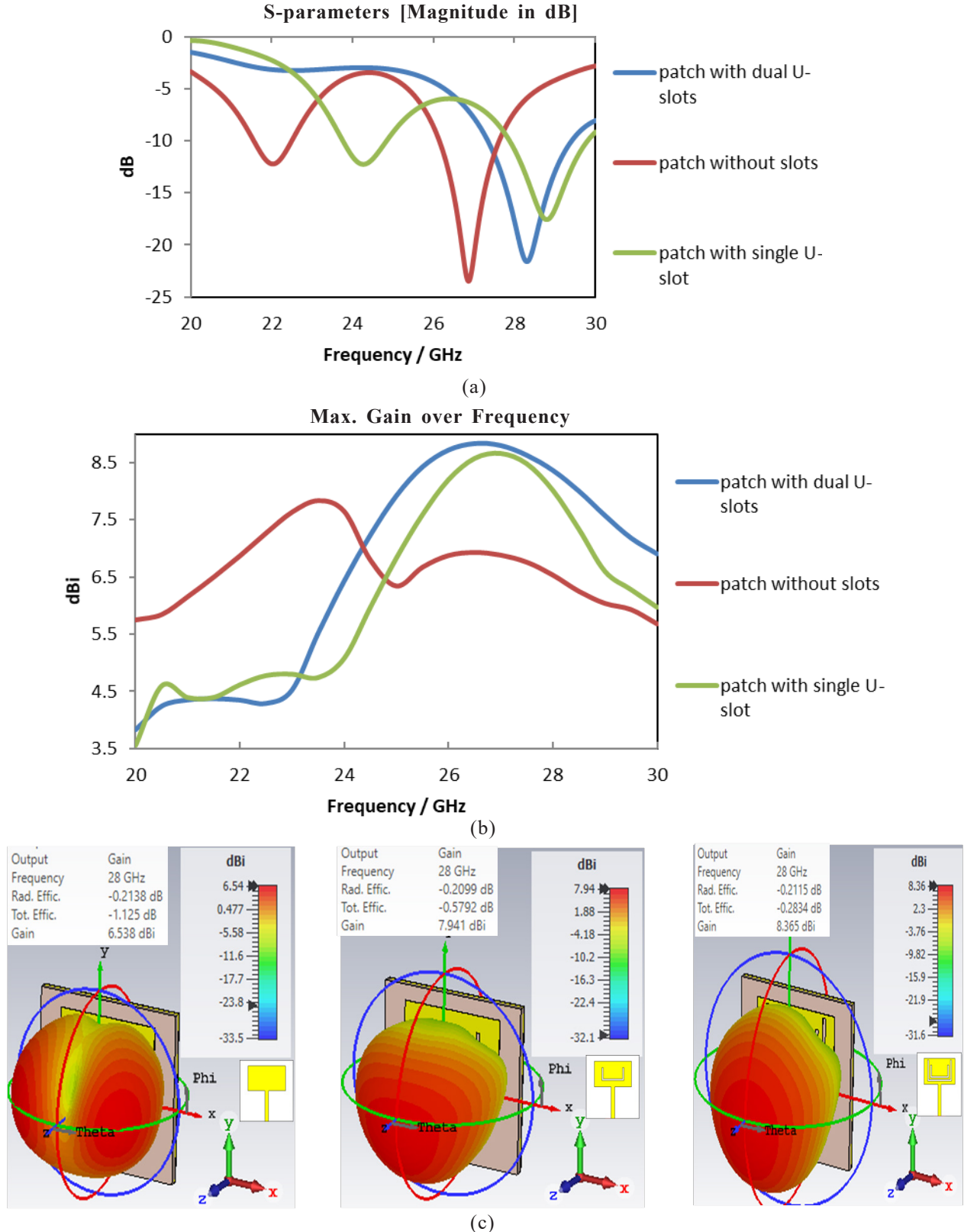
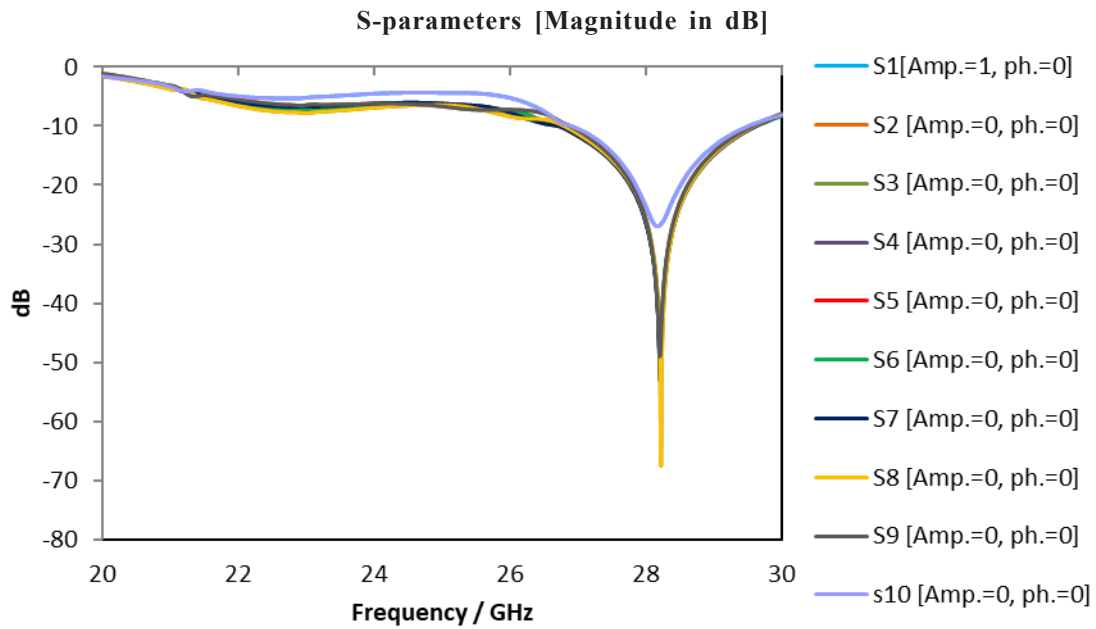
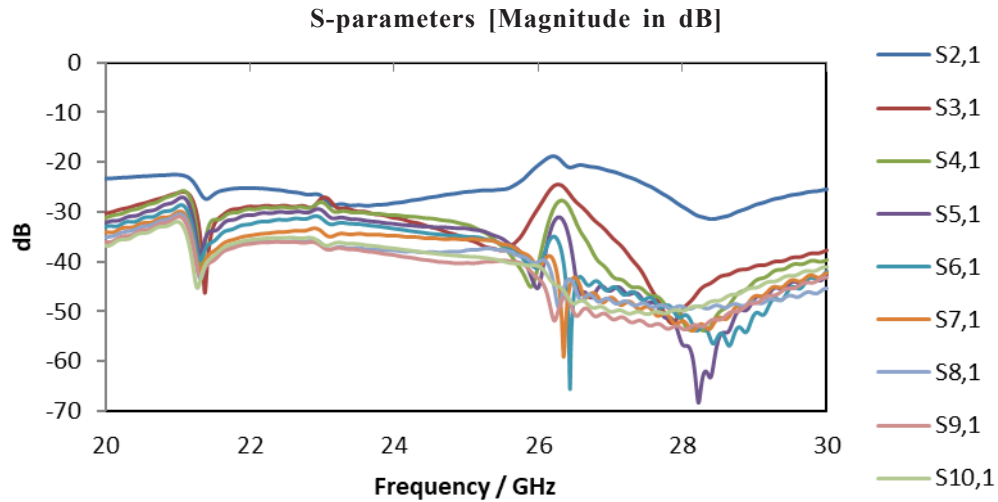


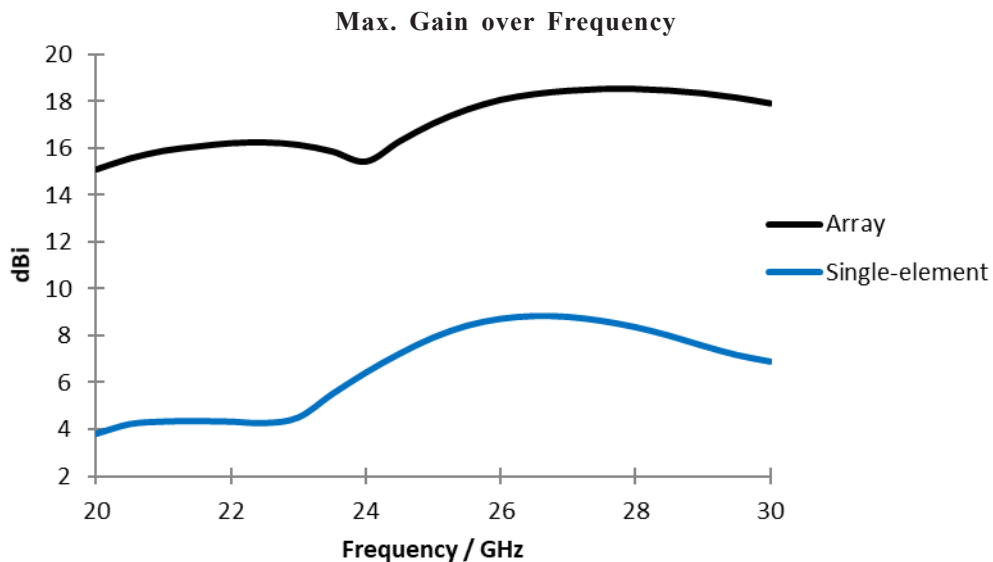
Figure 3. Simulated results of the single-element antenna; (a) Scattering parameters of the single-element antenna; (b) Peak gain; and (c) 3D radiation pattern.



(a)

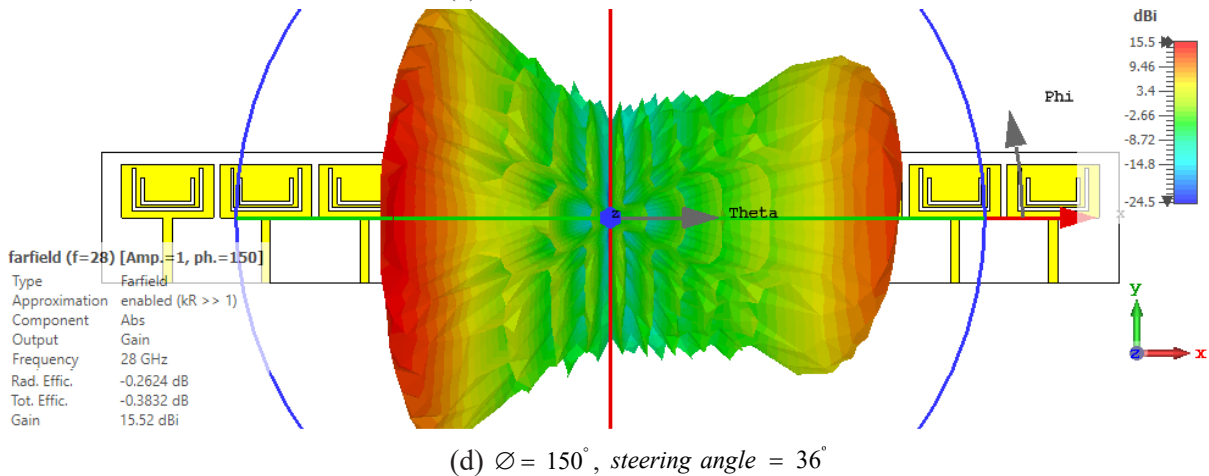
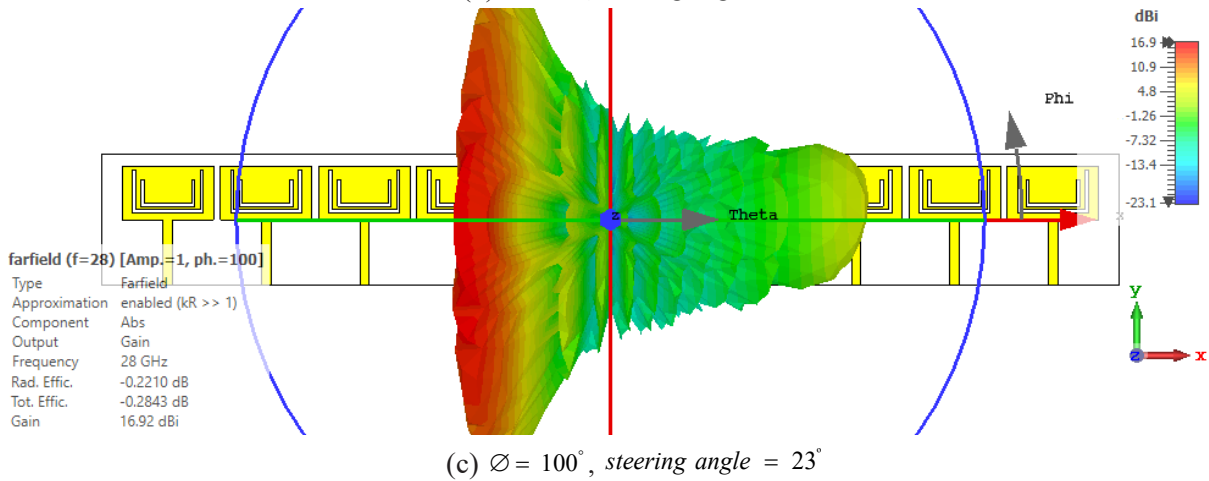
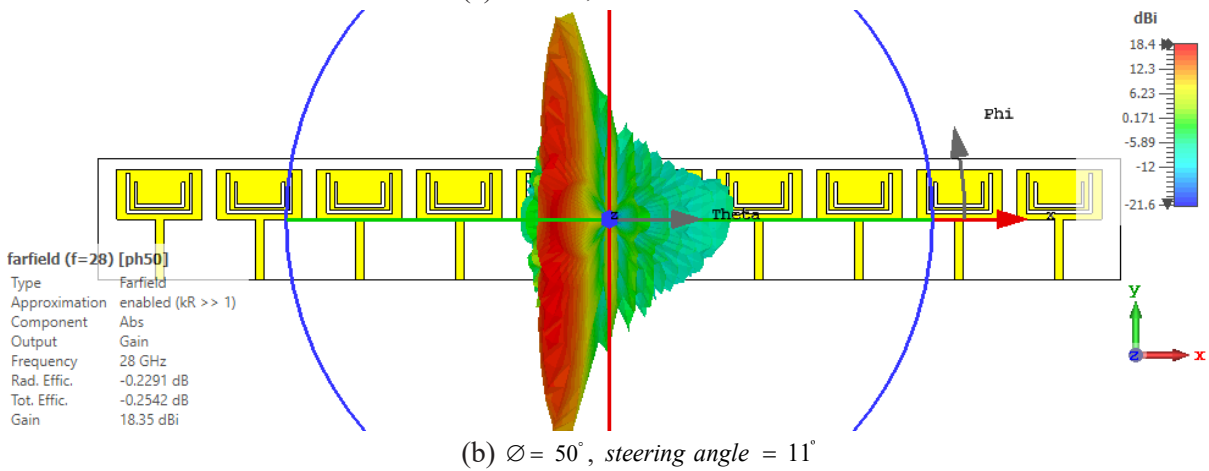
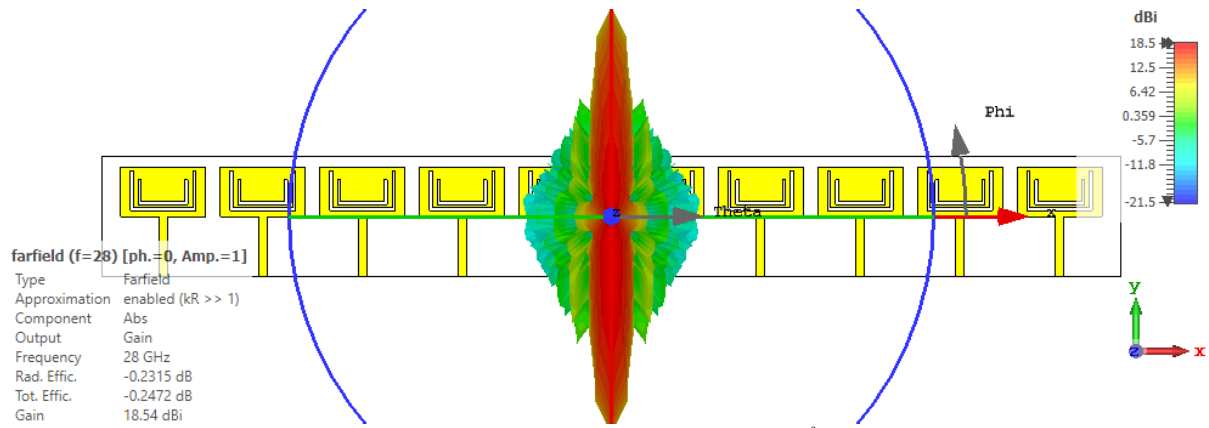


(b)



(c)

Figure 4. Simulated results of the proposed array antenna; (a) Scattering parameters; (b) Isolation; (c) Peak gain.



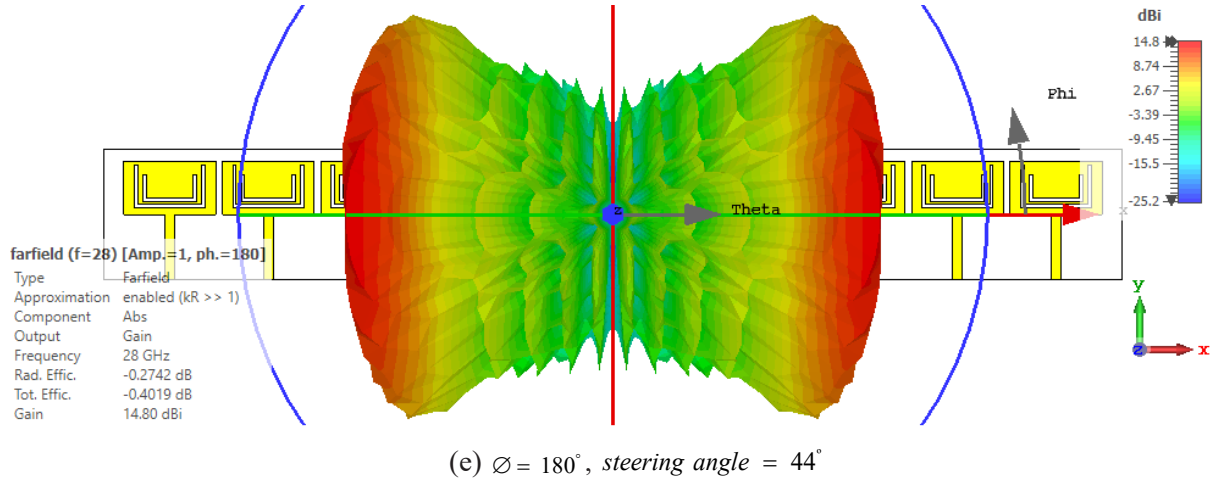


Figure 5. The 3D radiation patterns in the 28 GHz band at different phase shifts.

Table 3. Beam- steering investigation

Phase shift (deg)	Steering angle (deg)	Gain (dBi)	Directivity (dBi)	Realized gain (dBi)	Rad. Effic., Tot. Effic. (%)
0	0	18.5	18.8	18.5	95, 95
±50	±11	18.4	18.6	18.3	95, 94
±100	±23	16.9	17.1	16.9	95, 94
±150	±36	15.5	15.8	15.4	94, 92
±180	±44	14.8	15.1	14.7	94, 91

4(a) shows the scattering parameter of the array antenna versus the frequency. The array elements exhibited low return losses, ranging from -27 to -67.5 dB at 28.2 GHz. The $|S_{11}|$ parameter of the first and last elements was approximately -27 dB, while the remaining eight elements had values between -49.4 dB and -67.5 dB. These differences in the reflection coefficients are due to the mutual coupling between the elements, which affects the return loss response of the array. The reflection coefficient results revealed that the proposed array design provides a -10 dB bandwidth covering 26.7–29.6 GHz, allowing for frequencies beyond the 27.5–28.35 GHz band. The isolation between the array elements was less than -30 dB at 28.2 GHz, as shown in Fig. 4(b).

The peak gain characteristics of the single-element and array antennas were compared over frequency, as shown in Fig. 4(c). This figure shows that the array boosted the gain from 8.4 dBi to 18.5 dBi at 28 GHz. Fig. 5(a) presents the combined 3D radiation pattern of the array elements, which was used to analyze the far-field radiation behavior of the proposed array. The array obtained a directivity of 18.8 dBi and a realized gain of 18.5 dBi, with a side lobe level of -13.4 dB in the theta ($\phi = 0^\circ$) direction. The array radiated at an angle of 0° at the theta ($\phi = 0^\circ$) plane, and 7° with -18.5 dB side lobe level at ($\phi = 90^\circ$). The radiation pattern clearly demonstrates excellent performance, with a radiation efficiency of nearly 95 % and an antenna efficiency that is also high. Despite interelement mutual coupling, which can affect overall radiation performance, the antenna array maintained the same efficiency level.

4.3 Beam Steering

Here, we present the results of our investigation into the beam steering capabilities of the proposed array. Figure 5

shows the 3D radiation patterns at different phase shifts, with the highest steering angle achieved at a phase shift of 180° as illustrated in Fig. 5(e). The array could cover angles from -44° to 44° in the theta ($\phi = 0^\circ$) direction. Table 3 compares the steering angles in terms of the four antenna parameters (gain, directivity, realized gain, and efficiency). The values of these parameters were highest at the broadside (main lobe angle = 0°) at the theta ($\phi = 0^\circ$) plane, as depicted in Fig. 5(a), but decreased as the steering process went on. This is due to the main beam expanding and attempting to reach one of the side lobes within the visible region, as shown in Fig. 5(b–e). The values continued to decrease until they reached their minimum at a phase shift of 180° , as demonstrated in Fig. 5(e), after which they began to increase again. Despite this decrease in the values of the far-field radiation parameters, the proposed array still achieved the highest steering angle, with a gain value of 14.8 dBi in the theta ($\phi = 0^\circ$) direction, as displayed in Fig. 5(e) and Table 3. The array also maintained a sufficient gain range of 14.8 to 18.5 dBi, with only 3.7 dB loss at 28 GHz. The directivity ranged from 15.1 to 18.8 dBi, and the realized gain ranged from 14.7 to 18.5 dBi, as clarified in Table 3. Additionally, it is clear from Fig. 5 and Table 3 that the radiation efficiency for the scanning angles ranges from 94 % to 95 %, and the antenna efficiency ranges from 91 % to 95 %. Overall, it is evident from this section that the radiation performance of the array is only slightly affected by the beam-steering technique.

5. COMPARISON WITH THE RECENT LINEAR ARRAY ANTENNAS AT 28 GHZ

Table 4 compares the performance of the proposed array antenna with that of the recently published linear array antennas

Table 4. Comparison of the proposed array antenna with some of the most recent linear array antennas at 28 GHz

Ref.	Year	No. of elements	Freq. (GHz)	Bandwidth (GHz)	Mutual coupling (dB)	Peak gain (dBi)	Steering-range	Gain loss (dBi)	Rad. eff., tot. eff. (%)
[12]	2020	8	28	1.79	-25.02	11.16	$\pm 48^\circ$	NA	NA
[18]	2021	8	28	1	-15	12.5	$0^\circ-70^\circ$	4.5	90, 90
[19]	2023	8	26, 28, 32, and 36	11	-16	12.5	$0^\circ-80^\circ$	1.5	95, 80
[14]	2020	10	28	2	NA	12.8	$-53^\circ-68^\circ$	3	NA, 75
[20]	2022	8	26–29	3	-20	14.4	$-70^\circ-70^\circ$	2.4	NA
[21]	2020	32	28,38	0.89, 0.99	-35	16.5, 15.35	$\pm 45^\circ$	NA	NA
[23]	2018	12	24–28	4	-21	16.5	$\pm 60^\circ$	NA	NA,85
Proposed	2023	10	28	3	-30	18.5	$\pm 44^\circ$	3.7	95,95

based on eight important antenna characteristics: number of array elements, operating band, 10-dB frequency bandwidth, mutual coupling, peak gain, scanning range, gain loss, and efficiency. This study holds great significance and can be easily understood. The proposed antenna has the highest gain and efficiency. Furthermore, the mutual coupling of the proposed array and the 32-element array is the lowest among the other array designs²¹. The 10-dB bandwidth of the proposed array is higher than or equals to the bandwidth shown in^{12,18,14,20}. The proposed 10-element array has a steering range similar to the 32-element array proposed in²¹. In addition, its steering coverage is higher than those of the arrays proposed¹⁸⁻¹⁹. This suggests that the proposed array design could address the challenges faced by 5G millimeter-wave communication systems.

6. CONCLUSION

In this paper, a high-gain 1×10 slotted microstrip patch-phased antenna array operating at 28 GHz is designed and simulated using CST Microwave Studio for 5G applications. The results of the recently published array designs are compared with the simulation results of the proposed array antenna. Both the single-element and array antennas achieved low return loss (≤ -10 dB). The transformation of the single-element into a 10-element array antenna boosted the gain from 8.4 to 18.5 dBi with high efficiency. The mutual couplings between the elements are less than -30 dB within the band of interest. The bandwidth of the array antenna is approximately 3 GHz, which fully covers the (27.5–28.35 GHz) 5G band. The phased array antenna offers good beam steering capability. It covers a spatial angle of 88° with a peak gain of 18.5 dBi. Because of its effective radiation performance and novel design, the proposed high-gain array antenna is a potential candidate for 5G mm wave communication applications.

REFERENCES

- Maharjan, J. & Choi, D.Y. Four-element Microstrip patch array antenna with corporate-series feed network for 5G communication. *Int. J. Antennas Propag.*, 2020, 1-12, 8760297. doi:10.1155/2020/8760297
- Lee, H.; Kim, S. & Choi, J. A 28-GHz 5G phased array antenna with air-hole slots for beam width enhancement. *Appl. Sci.*, 2019, **9**, 1-11, 4204. doi:10.3390/app9204204.
- Sethi, W.T.; Ashraf, M.A.; Ragheb, A.; Alasaad, A. & Alshebeili, S.A. Demonstration of the millimeter wave 5G setup employing a high-gain vivaldi array. *Int. J. Antennas Propag.*, 2018, 1-12, 3927153. doi: 10.1155/2018/3927153.
- Mabrouk, I.B.; Al-Hasan, M.; Nedil, M.; Denidni, T.A. & Sebak, A.R. A novel design of radiation pattern-reconfigurable antenna system for millimeter-wave 5G applications. *IEEE Trans. Antennas Propag.*, 2020, **68**(4), 2585–2592. doi: 10.1109/TAP.2019.2952607.
- Ozpinar, H.; Aksimsek, S. & Tokan, N.T. A novel compact, broadband, high gain millimeter-wave antenna for 5G beam steering applications. *IEEE Trans. Veh. Technol.*, 2020, **69**(3), 2389–2397. doi: 10.1109/TVT.2020.2966009.
- Nabil, M. & Faisal, M.M.A. Design simulation and analysis of a high gain small size array antenna for 5G wireless communication. *Wirel. Pers. Commun.*, 2021, **116**(2), 2761–2776. doi:10.1007/s11277-020-07819-9.
- Sodré jr, A.C.; Costa, I.F.; Santos, R.A.; Filgueiras, H.R.D. & Spadoti, D.H. Waveguide-based antenna arrays for 5G networks. *Int. J. Antennas Propag.*, 2018, 1-10, 5472045. doi:10.1155/2018/5472045
- Paola, C.D.; Zhang, S.; Zhao, K.; Ying, Z.; Bolin, T. & Pedersen, G.F. Wideband beam-switchable 28 GHz quasi-yagi array for mobile devices. *IEEE Trans. Antennas Propag.*, 2019, **67**(11), 6870–6882. doi: 10.1109/TAP.2019.2925189.
- Nigam, H.; Mathur, M.; Arora, M. & Singh, R. Enhancing the gain with multiple beams for a four-element phased array microstrip antennas using a rogers substrate material for 5G applications. *Mater. Today: Proc.*, 2020, **30**, 203–209. doi:10.1016/j.matpr.2020.06.103.
- Arizaca-Cusicuna, D.N.; Arizaca-Cusicuna, J.L. & Clemente-Arenas, M. High gain 4×4 rectangular patch antenna array at 28 GHz for future 5G applications. In *IEEE XXV International Conference on Electronics, Electrical Engineering and Computing (INTERCON)*, 2018, 1-4.

- doi: 10.1109/INTERCON.2018.8526451.
11. Kiani, S.H.; Ren, X.C.; Bashir, A.; Rafiq, A.; Anjum, M.R.; Kamal, M.M.; Din, B.U. & Muhammad, F. Square-framed T shape mmwave antenna array at 28GHz for future 5G devices. *Int. J. Antennas Propag.*, 2021, 1-9, 2286011.
doi:10.1155/2021/2286011.
12. Kim, S. & Choi, J. Quasi-yagi slotted array antenna with fan-beam characteristics for 28 GHz 5G mobile terminals. *Appl. Sci.*, 2020, **10**, 1-17, 7686.
doi:10.3390/app10217686.
13. Nayat-Ali, O.; El Mrabet, O.; Aznabet, M. & Khoutar, F.Z. Phased array antenna for millimeter-wave application. *In International Conference on Computing and Wireless Communication Systems (ICWCS)*, 2019.
doi: 10.4108/eai.24-4-2019.2284237.
14. Deng, C.; Liu, D.; Yektakhah, B. & Sarabandi, K. Series-fed beam-steerable millimeter-wave antenna design with wide spatial coverage for 5G mobile terminals. *IEEE Trans. Antennas Propag.*, 2020, **68**(5), 3366–3376.
doi:10.1109/TAP.2019.2963583.
15. Yerrola, A.K.; Ali, M.; Arya, R.K.; Murmu, L. & Kumar, A. High gain beam steering antenna arrays with low scan loss for mmwave applications. *Def. Sci. J.*, 2022, **72**(1), 67–72.
doi : 10.14429/dsj.72.17318.
16. Parchin, N.O.; Basherlou, H.J. & Abd-Alhameed, R.A. Dielectric-insensitive phased array with improved characteristics for 5G mobile handsets. *Prog. Electromagn. Res. M.*, 2020, **94**, 209–219.
doi:10.2528/PIERM20042108
17. Khan, J.; Sehrai, D.A. & Ali, U. Design of a dual band 5G antenna array with sar analysis for future mobile handsets. *J. Electr. Eng. Technol.*, 2019, **14**(2), 809–816.
doi:10.1007/s42835-018-00059-9.
18. Parchin, N.O.; Al-Yasir, Y.I.A. & Abd-Alhameed, R.A. Phased array 5G antenna design with petal-shaped beams and improved radiation coverage. 15th European Conference on Antennas and Propagation (EuCAP), 2021, 1-5.
doi: 10.23919/EuCAP51087.2021.9410938
19. Amar, A.S.I.; Parchin, N.O.; Alibakhshikenari, M.; El-Hennawy, H. & Darwish, M. Wide-scan phased array antenna design for broadband 5G cellular networks. *International Microwave and Antenna Symposium (IMAS)*, 2023, 91-94.
doi: 10.1109/IMAS55807.2023.10066922.
20. Shen, X.; Xue, K.; Tang, X. & He, Y. Miniaturized-wide scanning angle phased array using the EBG structure for 5G applications. *Int. J. Antennas Propag.*, 2022, 1-7, 8769164.
doi:10.1155/2022/8769164.
21. El Halaoui, M.; Canale, L.; Asselman, A. & Zissis, G. Dual-band 28/38 GHz inverted-F array antenna for fifth generation mobile applications. *Proc.*, 2020, **63**(1), 53.
doi:10.3390/proceedings2020063053.
22. Mahabub, A.; Rahman, Md.M.; Al-Amin, Md.; Rahman, Md.S. & Rana, Md.M. Design of a multiband patch antenna for 5G communication systems. *OJAPr.*, 2018, **6**(1), 1–14.
doi: 10.4236/ojapr.2018.61001.
23. Stanley, M.; Huang, Y.; Wang, H.; Zhou, H.; Alieldin, A. & Joseph, S. A capacitive coupled patch antenna array with high gain and wide coverage for 5G smartphone applications. *IEEE Access*. 2018, **6**, 41942–41954.
doi: 10.1109/ACCESS.2018.2860795.

CONTRIBUTORS

Mrs Thura Ali Khalaf obtained MSc degree in telecommunication engineering from the University of Nahrain, Baghdad, Iraq. She has been a PhD student in the Electrical and Electronics Engineering Department at the University of Gaziantep, Gaziantep, Turkey. Her current research interests include: Design and analysis of microwave antennas in the millimeter-wave frequency band. In the current study, she contributed to the design of a novel high-gain array antenna for millimeter-wave applications, analysed the results, and prepared the manuscript.

Prof. Gölge Ögücü Yetkin obtained PhD degree in electrical and electronics engineering from the University of Gaziantep, Gaziantep, Turkey and working as an Assistant Professor in the Electrical and Electronics Engineering Department at the University of Gaziantep. Her research interests include: Computational electromagnetics, the design and analysis of printed structures, the development of numerically efficient techniques for analysing microwave antennas, circuits, and metamaterial-based printed structures. In the current study, she supervised the findings of this research, verified the results, and approved the final manuscript.